Edited by Ralf Zimmermann and Luke Hanley

Photoionization and Photo-Induced Processes in Mass Spectrometry

Fundamentals and Applications

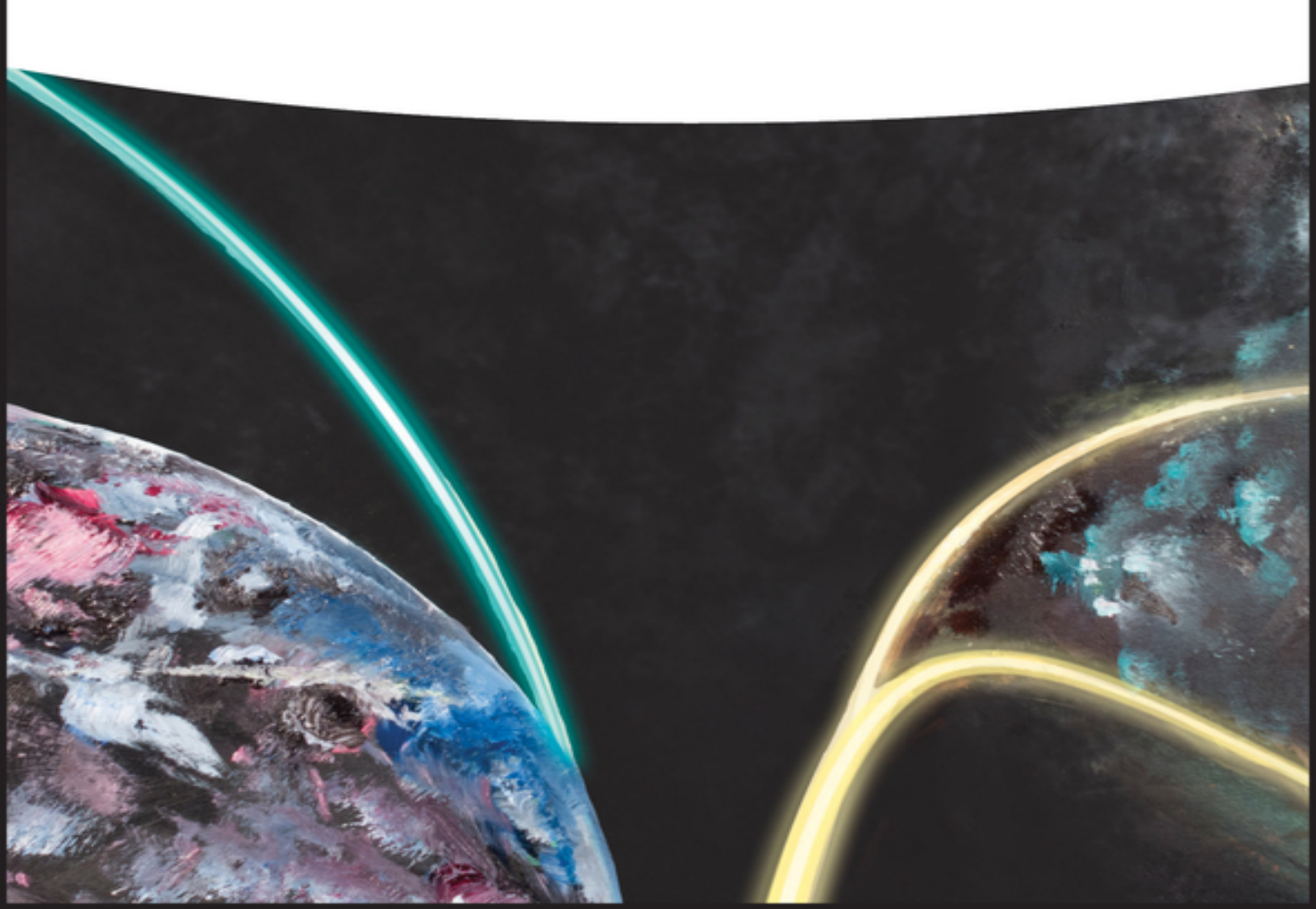


Table of Contents

Cover
<u>Preface</u>
1 Fundamentals and Mechanisms of Vacuum
<u>Photoionization</u>
1.1 Preface
<u>1.2 Light</u>
1.3 Photoabsorption
References
2 Fundamentals and Mechanisms of Resonance-
Enhanced Multiphoton Ionization (REMPI) in Vacuum
and its Application in Molecular Spectroscopy
2.1 Introductory Remarks
2.2 Beginnings of REMPI
2.3 Principle of REMPI: Rate Equations and
Quantification of Detection Efficiency
2.4 REMPI and Dissociation
2.5 Application of REMPI for Optical Spectroscopy
References
3 Analytical Application of Single-Photon Ionization
Mass Spectrometry (SPI-MS)
3.1 VUV Light Sources
3.2 Lamp-Based VUV Light Sources
3.3 Laser-Based VUV Light Sources
3.4 Mass Spectrometry with Lamp or Laser-Based
VUV Light Sources
3.5 On-line Analysis of Complex Mixtures by Single
Photon Ionization (SPI) Mass Spectrometry

3.6 SPI-MS in Hyphenated Applications
3.7 Ambient Monitoring
3.8 Commercial Solutions
References
4 Analytical Application of Resonance-Enhanced
Multiphoton Ionization Mass Spectrometry (REMPI-
<u>MS)</u>
4.1 Investigation of Model Flames
4.2 Applications to Internal Combustion Engines
4.3 Monitoring Combustion Process Emissions in an
<u>Industrial Environment</u>
4.4 Further Applications of REMPI Mass
<u>Spectrometry</u>
4.5 REMPI-MS in Hyphenated Analytical Systems
4.6 Commercial REMPI-MS Solutions and
<u>Applications</u>
<u>References</u>
5 Probing Chemistry at Vacuum Ultraviolet Synchrotron
<u>Light Sources</u>
5.1 Introduction
5.2 Combustion Chemistry
5.3 Isomer-Resolved Studies of Elementary
<u>Chemical Reactions</u>
5.4 Summary
<u>Acknowledgments</u>
References
6 Resonance Ionization Mass Spectrometry (RIMS):
Fundamentals and Applications Including Secondary Neutral Mass Spectrometry
Neutral Mass Spectrometry
6.1 Introduction

6.2 Resonance Ionization Fundamentals
6.3 Reduction to Practice
<u>6.4 Applications</u>
<u>6.5 Resources</u>
References
7 Ultrashort Pulse Photoionization for Femtosecond Laser Mass Spectrometry
7.1 Introduction
7.2 Mechanisms of Ultrashort Pulse Photoionization
7.3 Studies of Amino Acids, Dipeptides, and C60
<u>Leading to Advanced SFI Models</u>
7.4 Volumetric Intensity Dependence and Multiply
<u>Charged Ions</u>
7.5 Direct and Gas Chromatography-Coupled
Analysis of Explosives
7.6 Gas Chromatography-Coupled Analysis of Polyaromatic Hydrocarbons, Pesticides, and
Fragrances
7.7 Laser Secondary Neutral Mass Spectrometry
7.8 Conclusions
Acknowledgments
Disclosure Statement
References
8 Photoionization at Elevated or Atmospheric Pressure:
Applications of APPI and LPPI
8.1 Introduction
8.2 Atmospheric Pressure Photoionization
8.3 Low-Pressure Photoionization (LPPI)
8.4 Applications of APPI and LPPI
8.5 Conclusions

<u>Acknowledgments</u>
<u>References</u>
9 Fundamentals of Laser Desorption Ionization
9.1 Introduction
9.2 Experimental and Computational Parameters
and Observables
9.3 General Mechanistic Considerations
9.4 Laser-Induced Thermal or Acoustic Desorption
of Neutrals from Metal Surfaces
9.5 Molecular Resonantly Enhanced Desorption:
UV-MALDI and IR-LA
9.6 Nanophotonic Desorption
9.7 Femtosecond Laser Ablation
9.8 Internal Energy Transferred by LDI and
Supersonic Cooling
9.9 Conclusions
<u>Acknowledgments</u>
<u>Disclosure Statement</u>
<u>References</u>
10 Applications of Laser Desorption Ionization and Laser Desorption/Ablation with Postionization
10.1 Nature of Samples and Information to be Gained from Laser Desorption and Laser Ablation Mass Spectrometry
10.2 Laser Ablation and Laser Desorption Ionization MS for Elemental Analysis
10.3 Nonimaging MALDI-MS for Molecular Analysis 10.4 MALDI-MS Imaging for Molecular Analyses
10.5 Example of Standard MALDI-MS vs. Imaging

10.6 MALDI Alternatives: Matrix Free, Ambient,
Nanostructure Induced, and High Energy
10.7 Molecular LD/LA-MS Beyond Nanosecond UV
<u>Lasers</u>
10.8 Laser, Electrospray, and Other Postionization
of Plumes Formed by LD/LA
10.9 Laser Ablation Sampling for Solid or Liquid
<u>Collection</u>
10.10 Conclusions
<u>Acknowledgments</u>
<u>Disclosure Statement</u>
References
11 Laser Ionization in Single-Particle Mass
<u>Spectrometry</u>
11.1 Relevance of Atmospheric Aerosols for Climate
<u>and Health - The Single-particle Perspective</u>
11.2 Analysis of Individual Particles by Laser
<u>Ionization MS - Historical Development and Basic</u>
Principle 14 O. Frank and G. C.
11.3 Ionization in Single-Particle Mass
<u>Spectrometry: Laser Desorption/Ionization (LDI)</u>
11.4 Ionization in SPMS: Laser Photoionization of
<u>Previously Desorbed Species</u>
11.5 Instrumental Realizations
11.6 Data Evaluation
11.7 Applications
11.8 Commercial Laser Ionization Single-Particle
<u>Mass Spectrometry Systems</u>
References
<u>Index</u>
End User License Agreement

List of Tables

Chapter 1

<u>Table 1.1 Dipole selection rules for electronic transitions in a Hydrogen-lik...</u>

<u>Table 1.2 Typical oscillator strengths for transitions according to the selec...</u>

Chapter 2

<u>Table 2.1 The early beginnings of REMPI and</u> REMPI-MS.

<u>Table 2.2 The beginning of REMPI: early combinations with other techniques.</u>

<u>Table 2.3. (A) Calculated transition energies</u> <u>and</u> <u>further parameters (o...</u>

<u>Table 2.4 Assignment of the jet-cooled REMPI</u> <u>spectrum of biphenylene (left) a...</u>

Chapter 8

Table 8.1 Properties of the most typical dopants.

Table 8.2 Examples of APPI and LPPI applications.

Chapter 11

<u>Table 11.1 Important classes of aerosol particles,</u> their most abundant ions i...

<u>Table 11.2 Marker substances frequently used in SPMS, giving an indication on...</u>

<u>Table 11.3 Experimental photoionization schemes</u> <u>in SPMS, used mass analyzers ...</u>

List of Illustrations

Chapter 1

<u>Figure 1.1 Typical energy- and timescales of processes related to photoioniz...</u>

Figure 1.2 Illustration of a linearly polarized light wave as a so...

Figure 1.3 Behavior of the function $F(\omega, t)$ (Eq. (1.28)) that determines the time ...

Figure 1.4 Schematic wavefunctions (top) and their spectra (bottom). (a, d) ...

<u>Figure 1.5 Absorption spectrum of benzene, illustrating the dipole transitio...</u>

<u>Figure 1.6 Electronic transitions are faster than</u> <u>nuclear motion. The nuclei...</u>

<u>Figure 1.7 Ionization and fragmentation behavior of mescaline. (a) Electron ...</u>

<u>Figure 1.8 Ionization energies plotted against (a)</u> the molecular weight for ...

Figure 1.9 Single-photon ionization cross sections σ_{SPI} at 9.8 eV (0.4 eV FWHM)...

Chapter 2

<u>Figure 2.1 Schematic representation of the different possibilities of REMPI:...</u>

<u>Figure 2.2 A historically early demonstration of the two dimensionality of R...</u>

Figure 2.3 Typical energy level scheme of general REMPI process with first a...

<u>Figure 2.4 Ionization in an effusive molecular beam.</u>
<u>The ionization volume i...</u>

<u>Figure 2.5 Four different situations where the efficiency of REMPI is strong...</u>

Figure 2.6 (a) Wavelength ranges of molecular absorptions and typical transi...

<u>Figure 2.7 Comparison of one-color and two-color spectrum of naphthalene sho...</u>

<u>Figure 2.8 Two selected cases of problems due to an unfavorable overlap of v...</u>

Figure 2.9 Jablonski diagram with electronic states $(S_0, S_1, \text{ and } T_1)$ of the ...

<u>Figure 2.10 The case of 2,8 dichloro-dibenzofuran</u> as a textbook example for ...

<u>Figure 2.11 The effect of fast dissociation of the</u> intermediate resonant sta...

<u>Figure 2.12 The "ladder switching" mechanism of dissociative multiphoton ion...</u>

<u>Figure 2.13 REMPI mass spectrum of angiotensin</u> <u>for low (upper spectrum) and ...</u>

Figure 2.14 (a) REMPI-mass spectra of benzene in a highly mass-resolving ref...

<u>Figure 2.15 Effusive (room temperature) and</u> <u>supersonic gas beams for REMPI i...</u>

Figure 2.16 REMPI-spectra of effusive (room temperature) gas beams of (a) me...

<u>Figure 2.17 Mass-selected REMPI-UV-spectra (red lines) of three isomeric PAH...</u>

<u>Figure 2.18 Mass-selected (222 m/z) high resolution</u> <u>REMPI-UV-spectra of mole...</u>

Figure 2.19 (a) The biphenylene molecule: numbering and coordinate system. (...

<u>Figure 2.20 The REMPI spectrum of jet-cooled biphenylene. The spectrum depic...</u>

<u>Figure 2.21 Two-photon resonant, four-photon</u> <u>ionization REMPI spectrum (2 + ...</u>

Figure 2.22 Comparison of the vibronic structure of the S_1 -transition of tri...

Figure 2.23 (a) Jet-REMPI spectra of the S_1 -region of 1- and 2-monochlorodib...

<u>Figure 2.24 Selective ionization: REMPI spectra of jet-cooled chlorinated di...</u>

Figure 2.25 (A) Two-color REMPI spectrum of the S_1 -transition of [2.2]-parac...

<u>Figure 2.26 (a) REMPI mass spectra of para-xylene</u> in its natural carbon-isot...

<u>Figure 2.27 Two-laser beam setup to obtain ion currents from left- and right...</u>

<u>Figure 2.28 The flight time-to-position relation for a detuned time-of-fligh...</u>

<u>Figure 2.29 Twin-peak mass spectrum of the chiral molecule phenylethanol and...</u>

Figure 2.30 Procedure to determine a final *g*-value from the twin mass peak o...

Figure 2.31 Comparison of g values determined via CD-MS and $g_{\rm lit}$ values dete...

<u>Figure 2.32 REMPI-spectrum (a) and REMPI-PES</u> (b) of monofluorobenzene. (a) F...

<u>Figure 2.33 Steradiancy and time filters to</u> <u>selectively record ZEKE electron...</u> Figure 2.34 (a) Illustration of the lowering of the Coulomb potential thresh...

<u>Figure 2.35 (a) Typical time management of a MATI experiment. The time of io...</u>

Figure 2.36 (a) Set-up of an anion-ZEKE spectrometer. (b) The time managemen...

Chapter 3

Figure 3.1 Measured emission spectra of different VUV light sources in the w...

<u>Figure 3.2 (a) Setup of a VUV lamp-based SPI-ToF</u> mass spectrometer. In the d...

<u>Figure 3.3 Three mass spectra of a mineral oil-type fuel (diesel fuel, fully...</u>

<u>Figure 3.4 SPI mass spectra from different on-line measurement applications ...</u>

<u>Figure 3.5 Time profiles of selected masses from on-line SPI-MS measurements...</u>

<u>Figure 3.6 (a) Time-resolved SPI mass spectra,</u> normalized to the peak intens...

<u>Figure 3.7 Emerging gas-phase products from wood pyrolysis recorded by real-...</u>

<u>Figure 3.8 SPI mass spectrometry results</u> (PhotoTOF-process monitor, Photnion...

<u>Figure 3.9 Puff-to-puff resolved SPI-ToFMS</u> <u>measurement of cigarette smoke ge...</u>

<u>Figure 3.10 (a) The scheme of the cigarette mapping experiment – sampling ap...</u>

<u>Figure 3.11 Application of a mobile photoionization ion trap mass spectromet...</u>

Figure 3.12 (a) Two-dimensional comprehensive gas chromatogram (GC × GC) of ...

<u>Figure 3.13 Integration of a deuterium lamp to a ToF ion source for SPI (Jeo...</u>

Figure 3.14 (a) Setup of a direct inlet for liquid samples with photoionizat...

<u>Figure 3.15 (a) Experimental setup of the hyphenated instrument between ther...</u>

<u>Figure 3.16 SPI-MS of evolved gas analysis (EGA)</u> in thermal analysis (TA): r...

Figure 3.17 (a) Schematic diagram of a hyphenation between thermobalance and...

<u>Figure 3.18 Portable mass spectrometer with a membrane inlet system and a VU...</u>

Chapter 4

<u>Figure 4.1 Often applied laser types for REMPI and the respective laser wave...</u>

<u>Figure 4.2 (A) REMPI mass spectra of the emission of a hazardous waste incin...</u>

<u>Figure 4.3 Semiselective (top, 266 nm) and</u> <u>selective (bottom, 450 nm) REMPI ...</u>

Figure 4.4 (a) Sketch of the ion source for mass spectrometric detection of ...

<u>Figure 4.5 Application of the spectroscopic features</u> of REMPI for monitoring...

<u>Figure 4.6 (a) Experimental setup of Jet-REMPI-ToFMS apparatus . (b) Monitor...</u>

<u>Figure 4.7 (a) REMPI-MS monitoring of exhaust</u> <u>from a ship diesel engine (4-s...</u>

<u>Figure 4.8 First real-life field application of REMPI-ToFMS (1997) for on-li...</u>

Figure 4.9 Sketch of the components for indirect determination of I-TEQ valu...

<u>Figure 4.10 (A) Experimental setup for REMPI-ToFMS monitoring at a laborator...</u>

Figure 4.11 (a) Schematic depiction of the membrane inlet (MI) system for wa...

<u>Figure 4.12 First application of REMPI time-of-flight mass spectrometry as a...</u>

Figure 4.13 (a) Gas chromatograms of a mixture of three isomers of xylene an...

Figure 4.14 (A) Experimental setup used for (a) online concentration and de...

<u>Figure 4.15 (a) Photograph of the GC-APLI-ToFMS</u> <u>setup using a KrF excimer la...</u>

<u>Figure 4.16 (a) Instrumental setup of the direct infusion REMPI-MS and sampl...</u>

<u>Figure 4.17 (A) Instrumental setup of the hyphenation between a thermal/opti...</u>

Chapter 5

Figure 5.1 (a) 10.5 eV photoionization of spectrum and (b) 70 eV electron im...

Figure 5.2 Photoionization efficiency spectrum of C_3H_4 \pm , showing the dif...

<u>Figure 5.3 (a) Schematic diagram of pyrolysis apparatus with molecular beam ...</u>

<u>Figure 5.4 (a) Photoionization mass spectra taken</u> at 1380 K in the pyrolysis...

<u>Figure 5.5: Experimental (symbols) and simulated</u> <u>mole fraction profiles (lin...</u>

<u>Figure 5.6 Schematic diagram of the SVUV-PIMS</u> <u>JSR oxidation apparatus at NSR...</u>

<u>Figure 5.7 A mass spectrum taken from the JSR oxidation of *n*-butane at the p...</u>

<u>Figure 5.8 Mole fraction profiles of *n*-butane in its JSR oxidation at the pr...</u>

<u>Figure 5.9 Schematic diagrams of SVUV-PIMS</u> <u>premixed flame apparatuses at (a)...</u>

Figure 5.10 Mass spectrum of the premixed toluene/ O_2 /Ar flame ($\varphi = 1.90...$

Figure 5.11 Mole fraction profiles of (a) major flame species and (b) severa...

Figure 5.12 PIE spectra of m/z = 72, 58, and 44 in fuel-rich premixed flames...

<u>Figure 5.13 (a) Photograph of the combustion</u> <u>apparatus. (b) The vertical cut...</u>

Figure 5.14 Experimental mole fraction profiles of (a) ethylene, (b) O_2 , (c)...

<u>Figure 5.15 Schematic diagram of the coflow diffusion flame apparatus used a...</u>

<u>Figure 5.16 Measured mole fraction profiles of (a) toluene, (b) phenylacetyl...</u>

<u>Figure 5.17 Schematic diagram of biomass</u> <u>pyrolysis apparatus (Weng et al. 20...</u>

<u>Figure 5.18 (A) Photoionization mass spectra of the pyrolysis products of po...</u>

Figure 5.19 A schematic of flash photolysis slow-flow reactor depicting loca...

<u>Figure 5.20 Detection of the Criegee intermediate</u> by its PIE.

<u>Figure 5.21 10.5 eV photoionization mass spectrum of dimethyl ether pyrolysi...</u>

Figure 5.22 A schematic of the new instrument showing the locations of the p...

Figure 5.23 (a) Formation of C_5H_6 (m/z = 66) measured at 11.25 eV for the C_2

Figure 5.24 The measured values of k_1 st as a function of reactant density fo...

Figure 5.25 Photoionization energy spectra of the C_4H_4 and C_5H_6 products for...

<u>Figure 5.26 Summary of isomer-resolved product</u> <u>branching ratios for 1-butene...</u>

<u>Figure 5.27 Threshold photoelectron spectrum of the 1,3-butadiene and 2-buty...</u>

<u>Figure 5.28 Overview of aerosol chemistry and systems studied at the Chemica...</u>

Figure 5.29 SVUV aerosol mass spectrometer located at the Chemical Dynamics ...

Figure 5.30 10.5 eV Aerosol mass spectrum of squalane ($C_{30}H_{62}$) aerosol befor...

Figure 5.31 10 eV Aerosol mass spectrum of squalane aerosol coated with α-pi...

Figure 5.32 A 10 eV aerosol mass spectrum of flame-sampled particles from an...

<u>Figure 5.33 SVUV photoionization aerosol spectrum</u> <u>of squalane aerosol reacti...</u>

Figure 5.34 Effective uptake coefficients as a function of $[O_2]$ and $[Cl_2]$ in...

<u>Figure 5.35 Two-dimensional GC (GC × GC) setup</u> <u>using SVUV photoionization ma...</u>

<u>Figure 5.36 (a) 10.5 eV Photoionization mass</u> <u>spectrum of vehicular exhaust. ...</u>

<u>Figure 5.37 Chromatograms of selected ions for diesel fuel demonstrating the...</u>

<u>Figure 5.38 Positional carbonyl isomers resulting</u> <u>from the OH reaction with ...</u>

<u>Figure 5.39 Two-dimensional GC-SVUVMS selected</u> <u>ion chromatogram showing the ...</u>

Chapter 6

<u>Figure 6.1 Schematic diagram of a RIMS reflectron time-of-flight mass spectr...</u>

<u>Figure 6.2 Periodic table showing elements that</u> <u>either have been or could re...</u>

<u>Figure 6.3 Generic RIS schemes. (a) Two-photon</u> <u>excitation of an atom from th...</u>

Figure 6.4 A generic RIMS saturation curve in reduced variables. N_i/N_a is th...

<u>Figure 6.5 Allowed transitions and population distributions at equilibrium f...</u>

Figure 6.6 Gd RIS scheme in which no even isotopes (a) are ionized. Odd isot...

Figure 6.7 Hyperfine splitting and allowed transitions between J = 0 and J = ...

<u>Figure 6.8 Normalized number density along the</u> resonance laser direction of ...

<u>Figure 6.9 Sample pulsing scheme for secondary ion rejection in RIMS. The so...</u>

Figure 6.10 Useful yield for uranium sputtered from uranium oxide as a funct...

Figure 6.11 A collinear geometry RIMS system using a hot cavity ion source (...

Figure 6.12 (a) Secondary electron image of a SiC stardust grain pressed int...

<u>Figure 6.13 Simultaneous measurement of Fe and Ni isotopes avoiding the isob...</u>

Figure 6.14 (A) Two-photon RIS schemes for La, Er, and Eu using a common ion...

<u>Figure 6.15 A two-color RIS scheme for uranium that accesses both the ground...</u>

<u>Figure 6.16 (a) The populations of electronically excited D and F states of ...</u>

Chapter 7

<u>Figure 7.1 Schematic diagrams for the primary mechanisms associated with fem...</u>

<u>Figure 7.2 Keldysh parameter plotted as a function of the laser intensity (a...</u>

<u>Figure 7.3 Useful yield of valyl-valine photoions at various wavelengths and...</u>

<u>Figure 7.4 Ion intensity distribution of xenon for several charge states in ...</u>

Figure 7.5 Mass spectra of xenon when (a) the entire volume has been exposed...

<u>Figure 7.6 Mass spectra for 2,4,6-trinitrotoluene</u> (TNT) via GC-FLMS using (a...

<u>Figure 7.7 Displays example pesticides observed to display a variety of ioni...</u>

<u>Figure 7.8 Laser secondary neutral mass spectra</u> (SNMS) for sinapinic acid de...

Figure 7.9 Tryptophan fragments for all of the wavelengths studied ((a) 266,...

Chapter 8

<u>Figure 8.1 Standard configuration of an APPI orthogonal.</u>

Scheme 8.1 Ionization reactions in APPI (Kauppila et al. 2002; Syage 2004; K...

Scheme 8.2 Ionization reactions in negative ion APPI (Kauppila et al. 2004b)...

<u>Figure 8.2 LC separation of benzoin enantiomers</u> <u>using (a) APPI and (b) APCI....</u>

<u>Figure 8.3 (a) Schematic view of the</u> <u>microfabricated heated nebulizer from t...</u>

<u>Figure 8.4 Schematic of the capillary</u> <u>photoionization device connected to a ...</u>

<u>Figure 8.5 Schematic of the GC-APPI-Orbitrap</u> interface by Kersten et al. (a)...

<u>Figure 8.6 CE chromatograms using phosphate</u> <u>buffer for a three-drug mixture ...</u>

<u>Figure 8.7 Schematic of the desorption atmospheric</u> <u>pressure ionization (DAPP...</u>

<u>Figure 8.8 Drawing of an ambient insertion</u> <u>photoionization source that can b...</u>

Chapter 9

<u>Figure 9.1 Approximate timescales of nanosecond</u> and femtosecond energy absor...

<u>Figure 9.2 Calculated temperature rise (solid line)</u> on a gold surface induce...

Figure 9.3 Computer simulation of the time evolution of the first (S_1) and h...

Figure 9.4 (a) UV-MALDI-MS of phospholipids obtained from intact eye lens ti...

<u>Figure 9.5 fs-LA followed by 10.5 eV single-photon ionization of 2-methoxy-4...</u>

Chapter 10

Figure 10.1 Schematic configuration of laser ablation inductively coupled ma...

Figure 10.2 MALDI mass spectra of bovine serum albumin (BSA) tryptic peptide...

Figure 10.3 MALDI-MS imaging schematic workflow. Steps show the matrix appli...

<u>Figure 10.4 Schematic of laser desorption laser</u> <u>postionization (LDPI) MS. A ...</u>

Figure 10.5 ns-LDPI-MS image (1 × 1 cm) using 7.9 eV SPI shows the distribut...

Figure 10.6 One scheme for coupling LD/LA with electrospray ionization (ESI)...

<u>Figure 10.7 Schematic of laser ablation sample</u> transfer. Mid-IR laser is use...

Chapter 11

<u>Figure 11.1 Size modes and types of aerosols: (a)</u> <u>particle number size distr...</u>

- Figure 11.2 (a) Mortality during the "London smog event" 1952, modified from...
- <u>Figure 11.3 (a) Experimental setup of the LAMMA instrument, representing the...</u>
- <u>Figure 11.4 (a) Experimental setup of the single-particle mass spectrometer ...</u>
- <u>Figure 11.5 The basic design of current SPMS-MS instruments: particles enter...</u>
- <u>Figure 11.6 Typical timescales of basic physical processes in LDI. Blue: lig...</u>
- <u>Figure 11.7 Intensity thresholds for cation formation as a function of wavel...</u>
- <u>Figure 11.8 Intensity-dependent ion yields (a) for oleic acid particles of 6...</u>
- Figure 11.9 (a) Correlations between hourly mass concentrations for organic ...
- <u>Figure 11.10 Schematic of the working principle of</u>
 (a) laser desorption phot...
- <u>Figure 11.11 A very versatile and complex optical</u> <u>setup for LD-SPI in SPMS w...</u>
- <u>Figure 11.12 Exemplary mass spectra of two-step photoionization in SPMS. (a)...</u>
- Figure 11.13 (a) Multistep laser pulse sequence for combined LD-REMPI and LD...
- Figure 11.14 (a) Positive and negative ions from LDI combined with PAHs can ...
- <u>Figure 11.15 Schematic view of a dual-polarity Z-configuration time-of-fligh...</u>
- Figure 11.16 Schematic of an aerodynamic lens inlet system. At a pressure of...

<u>Figure 11.17 Calculated relative intensity</u> <u>distribution of Mie-scattered lig...</u>

Figure 11.18 Ternary plots showing the signal intensity of (a) secondary sul...

Figure 11.19 Composition of background aerosol (a) and cloud residuals (b) d...

Figure 11.20 The time evolution of anion mass spectra indicates the formatio...

Figure 11.21 SPMS-based detection of ships running on bunker fuel. (a) Avera...

Photoionization and Photo-Induced Processes inMass Spectrome

Fundamentals and Applications

Edited by

Ralf Zimmermann Luke Hanley

WILEY-VCH

Editors

Ralf Zimmermann

Helmholtz Zentrum München Institut für Ökologische Chemie Ingolstädter Landstr. 1 85764 Oberschleißheim Germany

Luke Hanley

University of Illinois

Department of Chemistry

United States

Cover Images: Courtesy of Jonathan Aldrich, The University of Illinois at Chicago

All books published by **Wiley-VCH** are carefully produced. Nevertheless, authors, editors, and publisher do not warrant the information contained in these books, including this book, to be free of errors. Readers are advised to keep in mind that statements, data, illustrations, procedural details or other items may inadvertently be inaccurate.

Library of Congress Card No.:

applied for

British Library Cataloguing-in-Publication Data

A catalogue record for this book is available from the British Library.

Bibliographic information published by the Deutsche Nationalbibliothek

The Deutsche Nationalbibliothek lists this publication in the Deutsche Nationalbibliografie; detailed bibliographic data are available on the Internet at http://dnb.d-nb.de>.

© 2021 WILEY-VCH GmbH, Boschstr. 12, 69469 Weinheim, Germany

All rights reserved (including those of translation into other languages). No part of this book may be reproduced in any form – by photoprinting, microfilm, or any other means – nor transmitted or translated into a machine language without written permission from the publishers. Registered names, trademarks, etc. used in this book, even when not specifically marked as such, are not to be considered unprotected by law.

Print ISBN: 978-3-527-33510-7 **ePDF ISBN:** 978-3-527-68223-2 **ePub ISBN:** 978-3-527-68222-5

oBook ISBN: 978-3-527-68220-1

Cover Design: Wiley

Preface

The goal of this book is to explain the fundamentals of photoionization (PI) and the associated applications of PI that are playing an increasingly important role in mass spectrometry (MS). The target audience of this book includes practicing scientists, including PhD and MSc students, whose primary interest is in the application of PI to elemental or molecular analysis by mass spectrometry. An overly simplistic analysis provides several motivations for the use of PI in mass spectrometry:

- 1. Enhance ion yields for specific important compounds of substance classes where other ionization strategies have proven insufficient,
- 2. Selectively ionize individual molecular structures or classes of molecules from mixtures,
- 3. Form ions from neutrals with reduced or controlled degree of fragmentation, and
- 4. Induce desorption or ablation of solids for sampling.

Photoionization comes in different versions and technological realizations, making it somewhat more complicated and thus less popular than standard ionization methods in mass spectrometry such as electrospray ionization and electron ionization. Nevertheless, one goal of this book is to demonstrate how these and other motivations drive the use of PI in MS-based analyses. The editors and authors hope that the readers will use this work as a series of building blocks for future advances in this promising area.

Actually, PI was central to the early development of mass spectrometry and single photon ionization (SPI) remains perhaps the best method for introducing a well-defined amount of internal energy into a molecular ion. Early work in SPI used vacuum ultraviolet (VUV) gas discharge lamps. However, the advent of lasers and the associated nonlinear optical methods made multiphoton ionization (MPI) possible, dramatically expanding PI as a fundamental strategy to probe molecular structure. The continuing improvement of laser technology has also created ongoing opportunities for MS-based applications of PI. For example, MPI via the excimer laser-pumped dye laser was deployed in many early fundamental studies, but was costly, difficult to use, and relatively unreliable. However, the development of smaller and rugged, field-deployable laser sources, such as compact excimer lasers, solid-state lasers as Nd:YAG lasers with integrated harmonic generation, and tunable solid-state lasers such as sealed, Nd:YAG-pumped optical parametric oscillators (OPOs) or Ti:sapphire cavities rendered MPI sufficiently robust for more widespread MS applications.

This interplay between fundamental methods and instrumental considerations has driven the development of analytical applications of PI, so attention is paid here to both considerations. Photodissociation is only discussed here when it occurs in conjunction with PI, such as via the formation of fragment ions from neutral precursors during MPI or SPI. Thus, the burgeoning use of photodissociation of the precursor or molecular ions to form fragment ions for structural elucidation of the former is not discussed here. The fundamentals and mechanisms of low pressure, gas-phase molecular PI for mass spectrometry is covered in Chapters 1, 2, 5, and 7, while molecular atmospheric pressure PI is a topic in Chapter 8. Applications and experimental methods of low-pressure, gas-phase

photoionization mass spectrometry (PIMS) are presented in <u>Chapters 3</u>, <u>4</u>, and <u>7</u>. Elemental analysis by PI is covered exclusively in <u>Chapter 5</u>. Processes and applications that include a laser desorption (LD) or direct laser desorption/ionization (LDI) of analytes from the condensed phase are covered in <u>Chapters 9</u> and <u>10</u>, while <u>Chapter 11</u> focuses on the direct analysis of individual aerosol particles using LDI, LD, and PI.

In the following, the content of the book is briefly highlighted chapterwise.

The first chapter entitled *FUNDAMENTALS* and *MECHANISMS* of *VACUUM PHOTOIONIZATION*, is serving as an introduction to mechanistic issues common to PI of molecules, atoms, and clusters under vacuum. It provides a fundamental description of light and the interaction of light and matter in the form of photoabsorption on a quantum mechanical level. This includes an excursion in perturbation theory and the dipole approximation and leads to an elucidation of the photon absorption selection rules. Finally, the SPI process, as an absorption in a continuum, nonbound state, is discussed and the most important parameters for SPI, the SPI cross sections and ionization energies, are deducted.

Fundamental aspects of MPI of molecules in the absence of gas-phase collisions are covered in the following chapter, entitled *FUNDAMENTALS* and *MECHANISMS* of *RESONANCE-ENHANCED MULTIPHOTON IONIZATION* (*REMPI*) in *VACUUM* and *APPLICATION* of *REMPI* for *MOLECULAR SPECTROSCOPY* (*Chapter 2*). Here, the theoretical consideration of photoionization processes is extended to MPI processes of molecular species and MPI-based spectroscopy, while multiphoton ionization of atoms is covered in *Chapter 6*. Different MPI and REMPI processes are presented and a rate equation approach is

used to deduct the influence of molecular physical properties on ionization efficiency. Special REMPI schemes are discussed, which can bypass unfavorable photophysical properties. In the following, MPI-induced fragmentation and dissociation processes are discussed. The application of REMPI for molecular spectroscopy with and without supersonic jet cooling is demonstrated in an exemplary manner via a detailed discussion of the REMPI wavelength spectrum of supersonic jet-cooled biphenylene and some other interesting aromatic molecules. REMPI wavelength spectroscopy, in particular with supersonic jet cooling, reveals the selectivity of the REMPI process that connects high-resolution ultraviolet (UV) spectroscopy to mass spectrometry. The selective ionization of isomeric and isobaric compounds, however, can be extended to the differentiation of isotopomers and - by using a special REMPI technique with circular polarized laser light - even of enantiomers. Finally, in this chapter, REMPI-based photoelectron spectroscopic (PS) techniques such as zero kinetic energy photoelectron spectroscopic (ZEKE-PS) are introduced. The explanation of the fundamental aspects of SPI and REMPI leads to the analytical application of these two PI approaches.

In the beginning of <u>Chapter 3</u>, which is entitled "ANALYTICAL APPLICATIONS of SINGLE-PHOTON IONIZATION MASS SPECTROMETRY," a brief introduction into common VUV-light sources, is given. These can be distinguished as incoherent light sources ("lamp"-based technologies) or coherent light sources (lasers). Also, a brief introduction to the generation of synchrotron light in the VUV range is elaborated (for applications of synchrotron-based SPI, see <u>Chapter 5</u>). The general setup of SPI mass spectrometry systems with laser- and lamp-based sources is introduced. Depending on the used VUV wavelengths, SPI can be a very soft ionization method,

enabling the detection of the molecular mass fingerprint of complex mixtures. This renders SPI-MS to an ideal approach for direct real time monitoring of complex gas and vapor mixtures. Different applications for online monitoring of combustion and pyrolysis processes are introduced, including online monitoring of gas phases from industrial processes, such as the coffee-roasting and/or the biomass pyrolysis process. Hyphenated instrumental analytical concepts, e.g. gas chromatography (GC) or thermal analysis (TA) coupled to SPI mass spectrometry, are presented and typical results are shown.

Chapter 4. "ANALYTICAL APPLICATION of RESONANCE-ENHANCED MULTIPHOTON IONIZATION MASS SPECTROMETRY (REMPI-MS), "gives, in a similar way as Chapter 3 for SPI, an overview of analytical applications of REMPI mass spectrometry. The preferential detection of aromatic analytes by the REMPI process with common laser is emphasized in <u>Chapter 3</u>. An overview on typical fixed-frequency laser lines (excimer lasers or frequencymultiplied, solid-state lasers) is provided along with typical wavelength ranges of tunable laser systems. In the following, several exemplary analytical concepts and applications using tunable and fixed-frequency lasers are presented. The tunable laser sources can be used to focus on specific analytes, which work particularly well with supersonic jet expansion inlet systems. For many applications, however, fixed-frequency wavelength laser and effusive, heated gas inlets can be applied for a useful and often very sensitive "overview" MS-profiling of many aromatic compounds. Exemplary process monitoring applications comprise detection of combustion by-products in flue gases of incineration plants or flavor and roast degree, indicating compounds in coffee-roasting off-gas. Hyphenated instruments connecting gas chromatography or a thermo-optical carbon analyzer (for aerosol loaded

filters) to REMPI-MS devices are discussed. A direct inlet of liquid samples into REMPI mass spectrometry is possible via a membrane inlet or a direct liquid introduction into the ion source. Note that SPI and REMPI processes can be performed in the same MS system. Finally, REMPI under atmospheric conditions is discussed (atmospheric pressure laser ionization – APLI; see also Chapter 8 for SPI-based atmospheric pressure-based ionization).

The application of synchrotron VUV light for SPI-MS-based investigation of combustion and pyrolysis processes is laid out in Chapter 5, "PROBING CHEMISTRY AT VACUUM ULTRAVIOLET SYNCHROTRON LIGHT SOURCES." By direct molecular beam sampling from flames as well as from oxidation or pyrolysis reactors, molecules from the reaction zone can be directly introduced in the mass spectrometer without wall contact. This enables the analysis of stable molecules and intermediates from the reaction zones. The flow reactors and model flame apparatus is often compact enough to be brought to synchrotron light source facilities and can be used for kinetic investigations. Unlike classical VUV sources, the synchrotron light from appropriate beamlines (i.e. equipped with VUV monochromators) exhibit a wide tunability, high energy resolution, and a relatively high photon flux. The identification of individual compounds from isobaric mixture components is possible by photoionization efficiency (PIE) spectroscopy, i.e. the recording of the ion yield as a function of the VUV wavelength. Chapter 5 also presents, an overview on different synchrotron-based PIMS apparatus and analytical results for several reactors and applications.

REMPI of atoms is commonly referred to as "resonance ionization mass spectrometry (RIMS). The RIMS technology and applications are described in the Chapter 6, RESONANCE IONIZATION MASS SPECTROMETRY